JOURNAL OF MATERIALS SCIENCE 23 (1988) 1289–1300

Viscoelastic dissipation and the tear energy of urethane–cross-linked polybutadiene elastomers

D. J. PLAZEK, G.-F. GU*
Department of Materials Science and Engineering, University of Pittsburgh, Pittsburgh, Pennsylvania 15261, USA

R. G. STACER‡, L.-J. SU§, E. D. VON MEERWALL, F. N. KELLEY
Institute of Polymer Science, The University of Akron, Akron, Ohio 44325, USA

A series of urethane–cross-linked polybutadiene elastomers of varying cross-linking levels have been investigated to determine the relationship between viscoelastic dissipation and tear (or fracture) resistance. Several points of correspondence were identified between these two properties. The first was an inverse proportionality in the terminal region between cross-link density and torsional creep behaviour as well as tear energy data, with the looser networks being more dissipative and displaying the greatest resistance to tear. Secondly, master curves of both creep compliance and tear energy exhibited a unique intermediate plateau. This plateau measured approximately 13 decades in time in each case. The temperature dependences were determined to be the same for the tear energy and creep compliance. Finally, in the terminal or long time region, it was found that the dynamic loss modulus G'' could be linearly correlated with the tear energy.

1. Introduction

The fracture and/or tearing of polymeric materials is usually determined by associated dissipative processes [1–7]. Only at relatively high temperatures ($T \gg T_g$), for slow rates of deformation when near equilibrium deformations are involved, does the nature and strength of the chemical bond play a determining role in the failure (tearing) process [8, 9]. However, the relationship between viscoelastic dissipation and tearing has remained relatively moot; i.e. it has not been clear how the tear energy is related to the viscoelastic relaxation and retardation spectra. It has been shown that the characteristic tear energy can be proportional to the imaginary component of the complex dynamic modulus (the loss modulus G'') [2] but the frequency dependence of G'' was not accounted for, thus leaving open the question whether different regions of the viscoelastic spectrum have different effects.

This question was addressed by measuring the fracture (tear) energies of several elastomers as functions of the temperature and rate of tear as well as their extended creep response. The variables studied were the molecular architecture which was varied by changing the cross-link density as well as the nature of the cross-linking.

The response of three fluorinated hydrocarbon elastomers (VITON) randomly cross-linked to different degrees have already been reported [10]. Three urethane cross-linked polybutadiene elastomers with differing cross-link densities are described in this paper along with a similarly cross-linked styrene–butadiene copolymer. Two polybutadiene polymers randomly cross-linked with dicumyl peroxide were also included in these studies.

2. Experimental procedure

The formulations of the six elastomers used as part of this study are given in Table I. Two types of liquid prepolymers were used to prepare the urethane cross-linked elastomers: one was R-45HT which is an approximately 2.5 functional hydroxyl-terminated polybutadiene (HTPB); the other was CS-15 which is hydroxyl-terminated styrene–butadiene copolymer (HTSBR) with a functionality of approximately 2.2. Both prepolymers were supplied by ARCO Chemical Company.

Two approaches can be used to control the cross-link density of polymer networks made from these materials. The first is to vary stoichiometrically the NCO/OH ratio of the cure system. This undercuring allows control over the number of network junctions but has the disadvantage of leaving unreacted–OH groups in the network junctions and provides a very broad distribution of chain lengths. A second approach was used as part of this study. The prepolymer was first endcapped by reacting it under nitrogen with toluene diisocyanate at an NCO/OH ratio of 2.0. This mixture was then cross-linked by the stoichiometric addition of a triol, trimethylolpropane. Control of cross-link density was obtained through

* *Permanent address:* Tung Chi University, Shanghai, People's Republic of China.
‡ *Present address:* Air Force Rocket Propulsion Laboratory, Edwards Air Force Base, California, USA.
§ *Present address:* General Tire and Rubber Company, Research Division, Akron, Ohio 44305, USA.

0022–2461/88 $03.00 + .12

TABLE I Formulations and properties

Ingredient or property	Units	Elastomer					
		HTPB-1	HTPB-2	HTPB-3	HTSBR	PB-1	PB-2
Hydroxyl-terminated polybutadiene (HTPB) ARCO R-45HT	g	62.27	63.06	62.44	–	–	–
Hydroxyl-terminated styrene butadiene (HTSBR) ARCO C-15	g	–	–	–	63.46	–	–
Polybutadiene aldrich	g	–	–	–	–	100	100
Trimethylol propane	g	23085	11689	0772	1843	–	–
1, 4-Butanediol	ml	–	1.1	1.5	–	–	–
Toluene diisocyanate	ml	7.14	7.23	7.16	5.7	–	–
Dicumyl peroxide	g	–	–	–	–	0.8	0.3
Butadiene microstructure*							
1, 4-*trans*	%	60	60	60	60		60
1, 4-*cis*	%	20	20	20	20		20
1, 2-vinyl	%	20	20	20	20		20
T_g†	°C	−79	−79	−79	−62	−102	−94
M_c‡	g mol^{-1}	3400	5200	8300	3900		3300

*From manufacturer's data.
†From differential scanning calorimetry.
‡From equilibrium modulus measurements.

use of a chain extender, 1, 4-butanediol, which was reacted prior to the addition of the triol. A suitable range of cross-link densities for the HTPB formulations was thus obtained, as shown in Table I.

Small deformation response characterization was accomplished using the torsional creep instrument of Plazek [11]. The rotating element in this apparatus is magnetically suspended and the torque is induced magnetically to maintain a very stable torque; therefore, the rotor touches nothing but the sample and is friction free. The angular strain of the torsion is measured by a light lever with a photocell recorder to achieve high angular resolution ($\sim 1.0 \times 10^{-5}$ rad).

The trouser tear test piece used to measure time-dependent fracture energies is shown in Fig. 1. The two arms of the test piece were separated at constant rates which are directly relatable to crack speed by a one-half factor [1]. Deformation of the legs was minimized through use of cloth backing, and the tear path was guided by a central slit extending nearly halfway through the thickness of the sample. Tear energies, τ, were then calculated from the tear force, F, and the width of the tear path, t, according to the equation

$$\tau = 2F/t \quad (1)$$

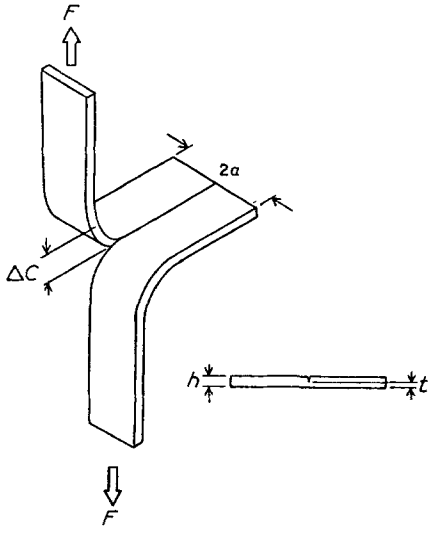

Figure 1 Trouser tear specimen. $T = 2F/t$ where $\lambda \simeq 1$.

3. Results and discussion

3.1. Creep behaviour of urethane cross-linked polybutadienes

Torsional creep measurements were made on the urethane–cross-linked polybutadiene elastomers at temperatures between −68 and 25° C. Illustrative reduced shear creep compliance curves $J_p(t) = J(t)(T_\varrho/T_0\varrho_0)$ for the intermediate cross-linked polybutadiene elastomer HTPB-2 are shown in Fig. 2 covering the time scale from about 1 sec to 1 day of creep. The temperature of reduction T_0 was chosen to be 0° C and ϱ_0 is the density at T_0. The $J_p(t)$ curves at the highest temperatures indicate an equilibrium compliance, J_e, at $T_0 = 0°$C of 1.0×10^{-6} Pa^{-1}. Results at lower temperatures indicate the presence of a well-defined plateau at a compliance which is about $1/3J_e$.

The reduced $J(t/a_T)$ curve obtained for the most loosely urethane–cross-linked polybutadiene HTPB-3 is shown in Fig. 3 where T_0 is 0° C, and a_T is the temperature-dependent shift factor. The lower cross-link density is reflected by a larger $J_e = 2.5 \times 10^{-6}$ Pa^{-1}. The plateau which is intermediate between the glassy compliance, J_g, (not reached in these measurements) and J_e, is most evident for this elastomer. The level of this plateau is about 2.0×10^{-7} Pa^{-1}.

To show the effect of network chain concentration on the response of the urethane–cross-linked polybutadienes the $J_p(t)$ curves for HTPB-1, -2 and -3 are presented in Fig. 4 reduced to $T_0 = 7.4$, 0 and 17.0° C, respectively. The reference temperatures were chosen so that the softening dispersions superpose (note that the order in temperatures does not correspond to the order of cross-link density). The network chain density obviously does not affect the form of the time-dependent response up to and including the intermediate plateau in the $J_p(t)$ curves. Only the terminal dispersion, i.e. the approach to J_e, is influenced.

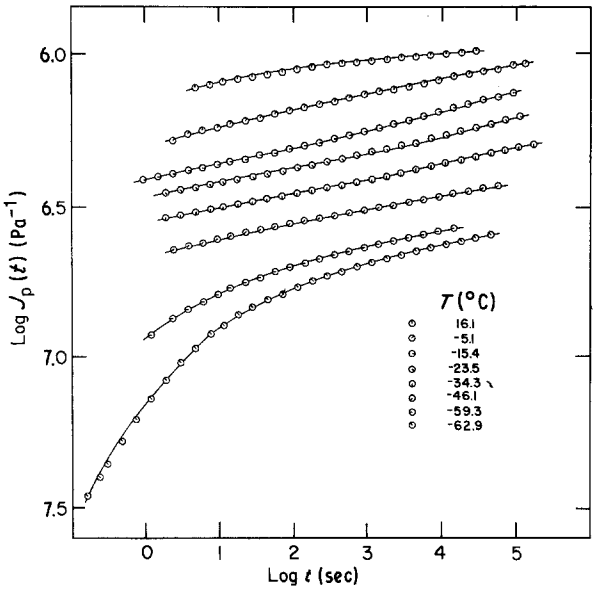

Figure 2 Log reduced shear compliance $J_p(t)$ plotted against log time, t for the urethane–end-linked polybutadiene HTPB-2 at various temperatures (°C). $J_p(t) = (T_0\varrho_0/T\varrho)\,J(t)$, where ϱ is the density at the temperature of measurement and ϱ_0 is the density at the reference temperature T_0.

The temperature-dependent shift factors, a_T, that were used to obtain the time scale reduced $J_p(t)$ curves of Fig. 4 are presented in Fig. 5 logarithmically as a function of the reciprocal absolute temperature (K^{-1}). Because they are given relative to the same $T_0 = 0°C$, the values of a_T are constrained to be equal to unity at $T^{-1} = 3.66 \times 10^{-3}\,K^{-1}$. The two features of these data surprising to a polymer rheologist are the linearity displayed and the order of the slopes of the lines. The linearity as a function of T^{-1} is not expected in the temperature range T_g to $T_g + 100°C$ because this is the range where changes in creep rates have been found to be determined largely by the volume, and therefore a response which can be fitted to the Williams, Landel and Ferry (WLF) equation is expected. This departure to the Arrhenius form appears to be unique in this temperature range and is attributed to the nature of the cross-linking units as will be illustrated below.

Reduced retardation spectra, L_p, calculated from the creep compliance curves [13, 14] shown in Fig. 4, are presented logarithmically in Fig. 6 as functions of the logarithmic reduced retardation time, τ/a_T. The chosen reference temperatures bring the short time spectral contributions together, showing the similarity between the networks of different chain density. The contributions to the terminal peak do indeed reflect the network topological differences. The more lightly cross-linked networks are markedly more dissipative at relatively longer times; i.e. in the time scale region populated by the mechanisms contributing to the long time or terminal peak in L. The objective measure of the width of the plateaus seen in the $J(t)$ curves is the separation of the peaks in L. These terminal peaks and their separations from the softening dispersion peak are remarkably large – 12 to 13 decades of time. Usually spectral peaks dominate a half dozen logarithmic units of the time scale and the separation of the terminal peak from the softening peak is a strong function of the network density [15, 16]. More systematic study of molecular variations will be necessary before an explanation of such mechanical spectra will be possible. However, the inverse relationship of viscoelastic dissipation at long times to network density as first seen in the response of natural rubber networks [15, 17] is confirmed phenomenologically even if it is not completely understood on a molecular level.

A most unusual reflection of the strange temperature-dependent time-scale shift factors, a_T, (displayed in Fig. 5) is seen in Fig. 7, where the $J_p(t)$ curves of the three urethane–cross-linked polybutadienes are shown all reduced to 0°C. At short reduced times ($\log t/a_T < -5$) it is seen that the positions of the softening dispersions do not correspond to the order of cross-link densities. As cross-linking increases T_g, at any given temperature the most highly cross-linked member of a series would be expected to creep most slowly (i.e. the $J(t)$ curve would be found at correspondingly longer times). In fact, the measured T_gs are the same within experimental uncertainty, $-79 \pm 1°C$. It appears, therefore, that the relative rates of creep at 0°C are determined principally by the temperature sensitivities indicated in Fig. 5. HTPB-2 has the greatest temperature sensitivity and therefore has the highest rate of creep in the range of the softening dispersion. HTPB-3 is the least temperature sensitive and creeps the slowest in the short time region. These last conclusions reflect the fact that

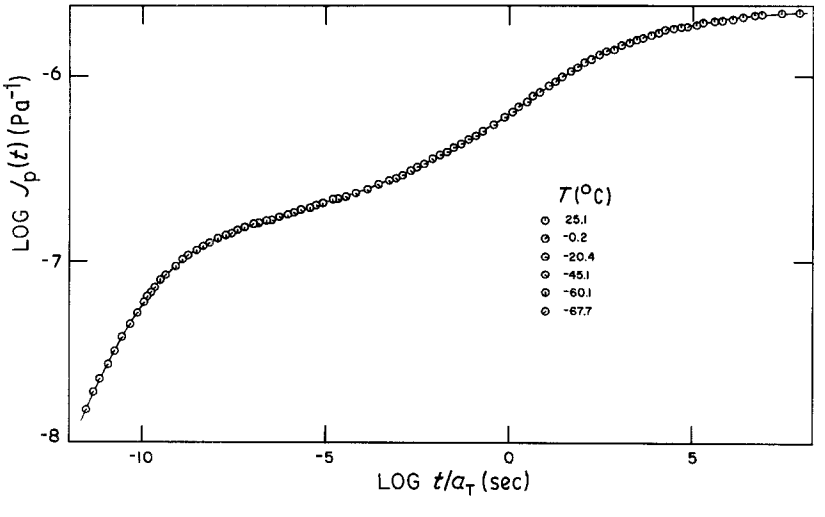

Figure 3 Logarithmic plot of the reduced shear creep compliance $J_p(t)$, of the doubly extended urethane–end-linked polybutadiene TB-3 against the logarithmic reduced time scale, t/a_T. The reference temperature of reduction, T_0, of 0°C.

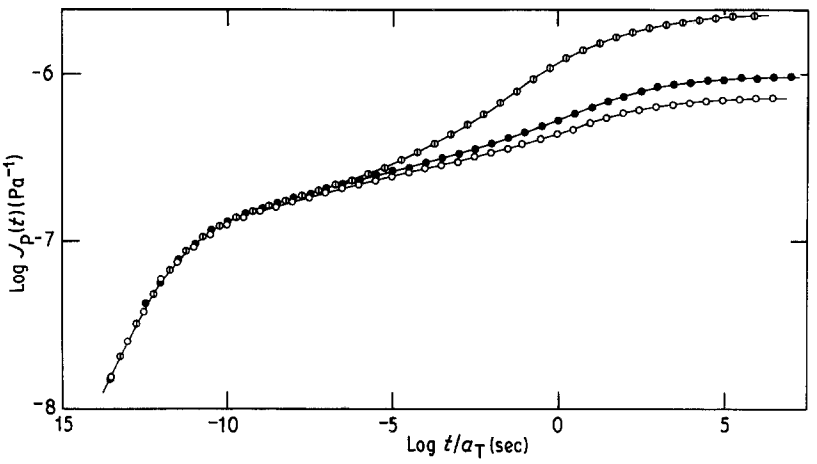

Figure 4 Logarithm of the reduced shear creep compliance, $J_p(t)$, for the three urethane–end-linked polybutadiene elastomers displayed as a function of the logarithm of the reduced time scale, t/a_T. Reference temperatures are chosen so that superposition is achieved at short times in the primary softening dispersion. (○) TB-1, 7.4° C, (●) TB-2, 0° C, (⊖) TB-3, 17.0° C.

at T_g the rates of creep in the softening transition are comparable.

It has been pointed out that it is not certain which viscoelastic function, if any, best describes the dissipations involved in mechanical deformations and their consequences [18]. Some investigators look to the loss tangent which reflects the relative magnitudes of dynamic loss moduli G'' (Pa) and compliances J'' (Pa^{-1}) to their storage counterparts G' and J'; i.e.

$$\tan \delta = G''/G' = J''/J' \qquad (2)$$

Reduced storage modulus curves of the end-linked elastomers are logarithmically presented in Fig. 8 along with the loss tangent curves. Dynamic compliances were calculated by means of numerical integration from L_p and moduli were obtained algebraically from the compliances. At the reference temperatures chosen to superpose the softening dispersions it is seen that sample differences in tan δ are greatest near the maxima and are minimal again in the low reduced frequency ωa_T region. If the corresponding loss modulus, log G''_p, curves in Fig. 9 are examined, it is seen that the modest differences (found in other functions) between samples HTPB-1 and HTPB-2 all but disappear and HTPB-3 shows the highest G''_p values

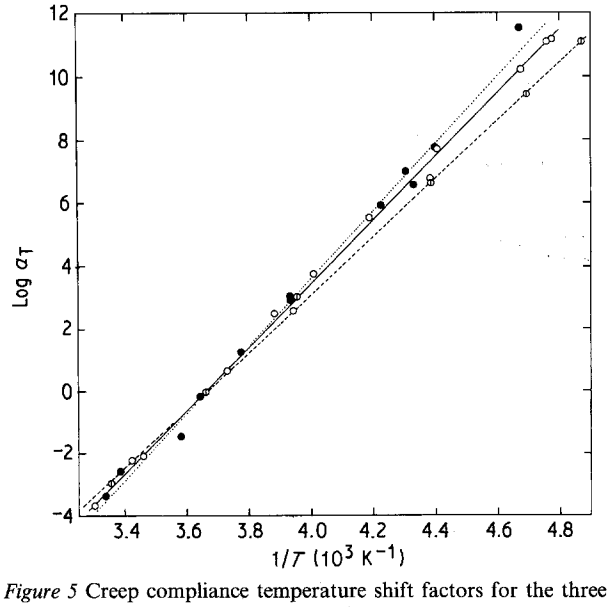

Figure 5 Creep compliance temperature shift factors for the three urethane–end-linked polybutadiene elastomers plotted logarithmically as functions of the reciprocal absolute temperature. a_T is defined to be equal to one at the reference temperature T_0 = 0° C. (○) HTPB-1, (●) HTPB-2, (⊖) HTPB-3.

at intermediate reduced frequencies, whereas its G''_p values at the lowest reduced frequencies are about one-third of those of the other samples. These observations will be referred to again after the fracture energy curves are presented.

3.2. Tearing of urethane–cross-linked elastomers

As previously mentioned, the exact relationship between the viscoelastic spectra and the tearing process remains in doubt. General trends have been observed and correlations drawn, but these are not wholly satisfactory. Part of this problem has arisen because of the experimental dificulties associated with tear measurements. Data scatter can be large and significant trends are often obscured. The general shape of the tear energy master curve over broad time scales has been found to be either linear with a positive slope [19, 20] or a gradual, monotonically increasing curve [2, 21, 22] when presented against reduced crack rate in log–log coordinates. Although it must be presumed that limits or plateaus exist at both the very long and very short time scales, plateaus observed in between these extremes are most often associated with regions of unstable tearing [23].

When tear tests are conducted at very low rates and at temperatures well above the T_g of the network polymer, they approach a limiting value defined as the threshold tear energy, τ_0. Lake and Thomas [24] derived a relationship which may be written

$$\tau_0 = KM_c^{\frac{1}{2}} \qquad (3)$$

where M_c is the average molecular weight of a network chain and K is a constant for the polymer which depends on the energy required to rupture the weakest chain bond; the density of the polymer; and the mass, length, and flexibility of the monomer unit. The exponent $\frac{1}{2}$ was derived by Lake and Thomas using rubber elasticity theory and a very simple model for the number of chains crossing the tear tip. King and Andrews [22], using a more realistic geometry, although still highly simplified, argued that the exponent should be 1/3, indicating a slightly lower dependency on M_c. It should be noted that the cubic model and argument used by King and Andrews had previously been employed by Beuche [25] to develop a 1/3 exponential relationship between the strength of an elastomer and M_c.

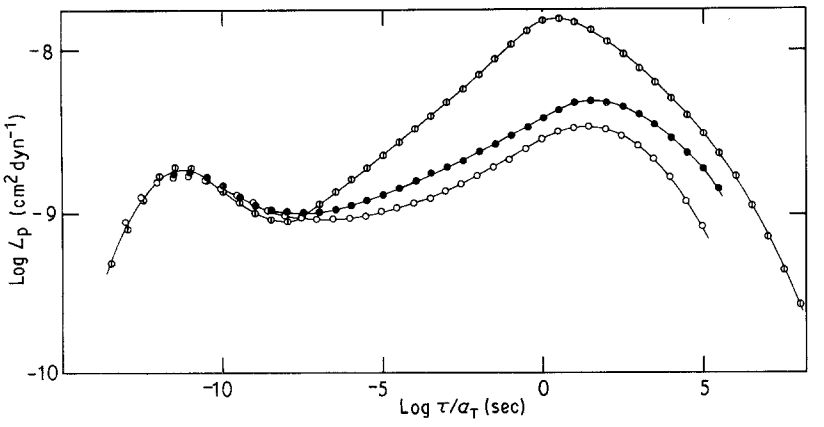

Figure 6 The logarithm of the reduced retardation spectrum, L_p, shown as a function of the logarithm of the reduced retardation times, τ/a_T, for the three urethane–end-linked polybutadienes (○) TB-1, (●) TB-2 and (⊖) TB-3. The response has been reduced to corresponding state temperatures of 7.4, 0 and 17.0° C, respectively for the primary softening transition.

Experimental investigations have generally supported a fractional power proportionality between network strength and M_c. Mullins [26] showed a linear relationship between ultimate strain capability and $M_c^{\frac{1}{2}}$ for natural rubber gum formulations. Smith and Chu [27], in an attempt to verify Bueche's theory, related ultimate stress capability at maximum network extension to $M_c^{0.4}$ for a series of fluorocarbon elastomers. Using highly cross-linked epoxy networks above their T_gs, King and Andrews' [22] attempts to measure τ_0 were inconclusive. The most extensive investigation to-date was that carried out by Gent and Tobias [28]. Systematically varying the cross-linking level in a series of five different elastomers, they were able to relate τ_0 to $M_c^{\frac{1}{2}}$. It should be noted, however, that data for some of the individual elastomers varied from the 1/2 exponent by statistically significant amounts.

Tear energy measurements were made on the urethane–cross-linked polybutadienes over a temperature range from − 65 to 72° C. Data were shifted using shift factors from the Arrhenius relationship illustrated in Fig. 5. Good super-position of the data was obtained even though unstable tearing was observed at lower temperatures. Use of the temperature-dependent vertical shift factor was not deemed necessary to obtain good superposition: however, this reduction factor was employed when direct comparisons were made between creep and tear data. In this case, the reduced tear energy is designated as τ_p.

In previous work with VITON elastomers [10], it was found that tear energy master curves could be conveniently described by one-half of a Gaussian distribution function in x, Y coordinates:

$$Y = P_3 + P_2 \exp - \left[\frac{(x - P_4)^2}{W}\right] \quad (4)$$

$x \equiv \log[\dot{C}a_T]$ where $\dot{C}$ is the crack velocity (m sec^{-1}) and a_T the temperature shift factor, and W is related to the half-width of the curve through

$$W = e^{\frac{1}{2}} 2^{\frac{1}{2}} \frac{P_2}{P_1} \quad (5)$$

Parameter P_3 is the asymptote of the curve and thus represents the threshold tear energy. $P_2 + P_3$ is the maximum of the curve as the tear energy nears T_g, P_1 is the maximum slope of the curve, and P_4 is the centroid x position. While this function is certainly not the only possible function which could have been used to describe the VITON data, it possesses the necessary attributes to provide discrete slope and position parameters of high significance if it fits the data reasonably. Its use may be considered as an *ad hoc* evaluation tool, to be well confirmed by statistical criteria.

Tear energy data for the urethane–cross-linked elastomers used in this study could not be modelled by Equation 4. A distinct intermediate plateau in these data required an equation with additional features. These features are incorporated using a power law equation for the plateau and a Gaussian distribution for the peak. This approach is illustrated in Fig. 10 and in the following equation

$$Y = P_7 + \frac{P_3}{1 + e^{(X-x)/m}} + (P_2 - P_3)e^{-[(x-P_6)/W]^2} \quad (6)$$

with

$$W = e^{\frac{1}{2}} 2^{\frac{1}{2}} \frac{P_2 - P_3}{P_4}$$

P_7 is the asymptote or threshold tear energy, P_1 and P_4

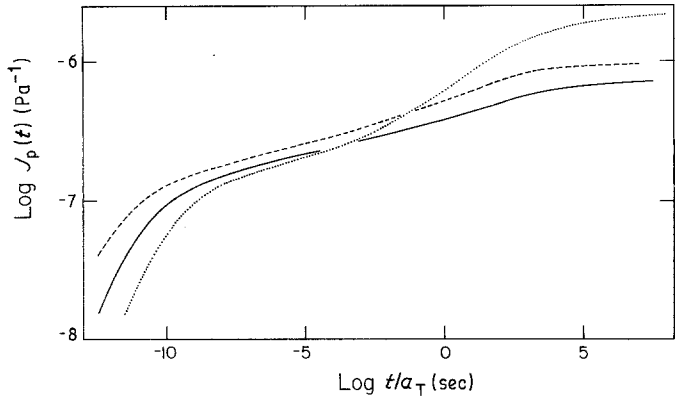

Figure 7 Logarithm of the reduced shear creep compliance, $J_p(t)$, for the three urethane–end-linked polybutadiene elastomers, (——) TB-1, (– – –) TB-2 and (· · ·) TB-3 plotted against the logarithm of the reduced time scale, t/a_T. All curves are reduced to a reference temperature, T_0, of 0° C.

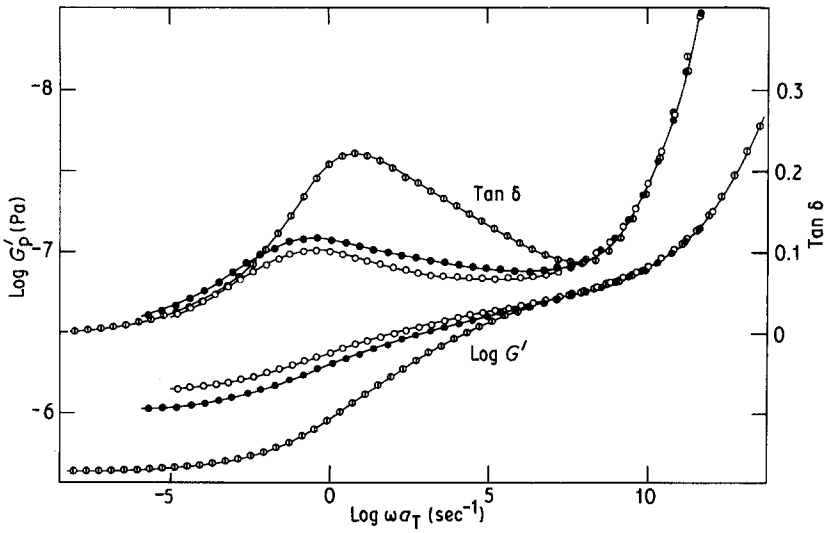

Figure 8 The loss tangent, tan δ and the logarithm of the reduced storage modulus, G'_p, presented as functions of the reduced frequency scale ωa_T, for the three urethane–end-linked polybutadienes (○) TB-1, (●) TB-2 and (⊖) TB-3. The response has been reduced to corresponding state temperatures of 7.4, 0 and 17.0° C, respectively, for the primary softening transition.

are the maximum slopes of the curves before and after the plateau, P_3 is the height of the peak in the glassy region, and P_5 and P_6 are the horizontal positions of the plateau and peak, respectively. X is the horizontal position at $x = P_1$ and can be determined, together with m, from P_1, P_3 and P_5. For the case where no plateau exists, P_3 will be zero and Equation 6 reduces to Equation 4.

Fig. 11 presents the tear master curves, referenced to the common T_g, for the HTPB series of elastomers with individual data points shown for HTPB-3. Application of Equation 6 is shown by the solid lines. The fit for these curves was excellent as indicated by reduced chi-square values of 0.58, 0.57 and 0.75 for the three HTPB elastomers in ascending order. As can be seen, all three curves are roughly parallel with tear strength appearing to be inversely related to network cross-link density in a fashion similar to the earlier discussed small deformation response data. The curves shown in Fig. 11 were all drawn so that they asymptotically approach τ_0, with $\tau_0 \propto M_c^{\frac{1}{2}}$. Measurements of τ_0 for the urethane networks HTPB-1 and HTPB-3, swollen in paraffin oil, were made by Tobias [29]. These were found to be 46 ± 7 and 62 ± 8 J m^{-2}, respectively, in good agreement with the values predicted by the Lake and Thomas theory. τ_0 was estimated from Equation 3 for the remaining elastomers used in this study. The curves in Fig. 11 show evidence of an intermediate tear energy plateau centred at approximately 10 K J m^{-2} for these urethane–cross-linked networks. Although not completely distinct, the width of the plateau was estimated at 13.5 decades of time for all the elastomers from parameters P_5 and P_6 of Equation 6. Agreement between this value and the peak separation distances measured from the retardation spectra (Fig. 6) was excellent. This agreement suggests a common origin for the plateaus.

In order to test whether additional correspondence exists between the creep and tear data, it was necessary to convert tear crack growth rate to strain rate, $\dot{\varepsilon}$. Strain rate, although difficult to determine precisely at the tip of a tear [19, 20, 30], has been approximated here from the relation

$$\dot{\varepsilon} \approx \dot{c}/t \qquad (7)$$

where $\dot{c}$ is the crack growth rate and t represents sample thickness.

Fig. 12 illustrates the relationship between shear loss modulus and tear energy. This plot was obtained by taking the loss modulus at a given frequency and determining the tear energy from the corresponding

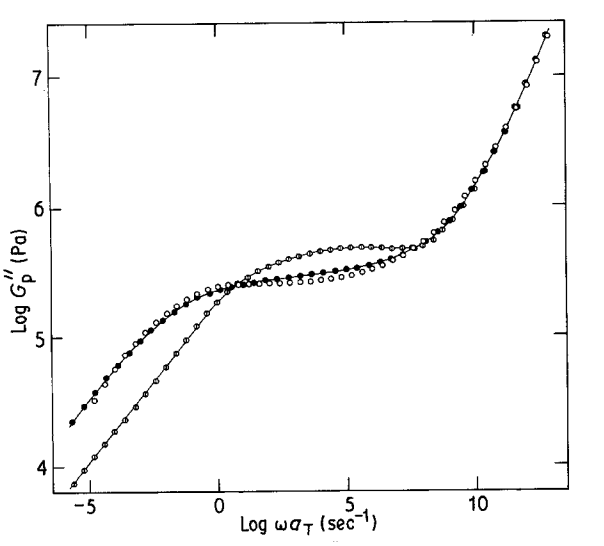

Figure 9 The logarithm of the reduced loss modulus, G''_p, plotted against the logarithm of the reduced frequency scale ωa_T, for the three urethane–end-linked polybutadienes (○) TB-1, (●) TB-2 and (⊖) TB-3. The response has been reduced to corresponding state temperatures of 7.4, 0 and 17.0° C, respectively, for the primary softening transition.

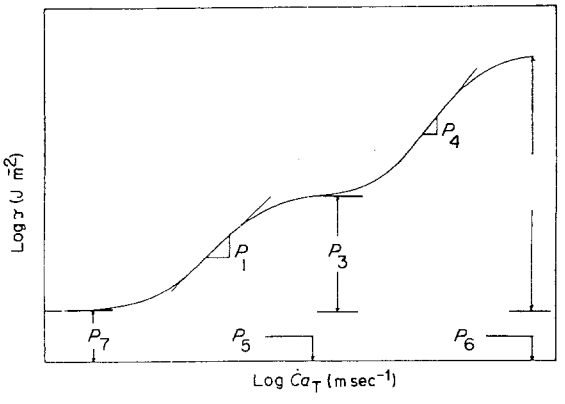

Figure 10 Schematic logarithmic tear energy curve as a function of a reduced logarithmic rate scale with identification of the seven parameters used in fitting.

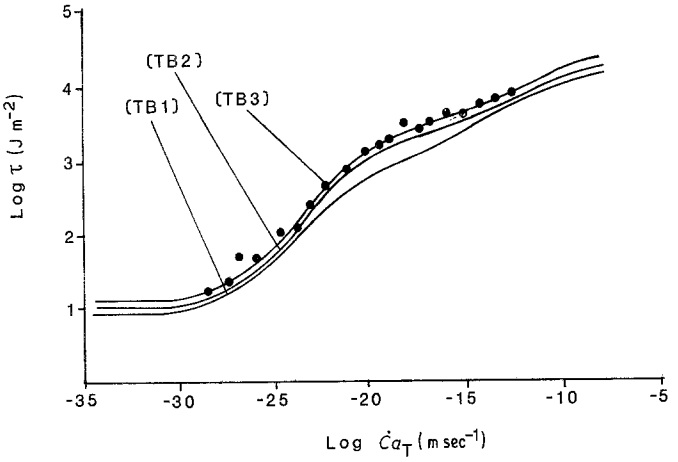

Figure 11 Double logarithmic plots of the tear energy, τ, against the reduced tear rate, $\dot{C}a_T$ for three HTPB elastomers. The reference temperature for reduction T_0 is $-79°C$ for all samples.

strain rate. As can be seen, good linear correlation exists only at low values of loss modulus and tear energy. The transition between the correlated and uncorrelated regions occurs at 1 sec for all three elastomers, agreeing with the onset of the intermediate plateau. At times shorter than 1 sec, tear energy increases more rapidly than would be predicted from G''. At longer times, the slopes of all three lines appear parallel. Differentiation between the individual slopes of the three cross-linking levels is more readily apparent when the data are replotted without the aid of a logarithmic transform (Fig. 12 inset). These slopes, designated β, have the units of lengths. The β values for the three elastomers in descending order of cross-link density are 11, 22 and 27 mm. Some linear correlation exists between β and M_c as illustrated in Fig. 13. In this figure, a best fit line with slope equal to one has been employed; however, this line does not fully describe all the data when individual error bars are considered. The exact origin of the variation of β with M_c is not clear at this time. One possible explanation may be related to tear tip diameter, with the looser networks having greater intrinsic tear tip diameters. Measured tear energy has been shown to be proportional to tear tip diameter [31] and tear tip diameter can be influenced by formulation changes [32]. A one-to-one relationship between β and tear tip diameter is not indicated, however because β is at least an order of magnitude greater than intrinsic tear tip diameters experimentally determined for other elastomers [20, 30].

Fig. 13 also shows the tear energies at $G''_p = 0$ plotted against M_c. These values should correspond to the threshold tear energies previously discussed because energy losses are assumed to be zero under threshold conditions. The extrapolated τ_0 energies from Fig. 12 are 49, 57 and 68 J m^{-2} for HTPB-1, HTPB-2 and HTPB-3, respectively. As can be seen in Fig. 13, agreement between these extrapolated values and those directly measured [29] is excellent. Additionally, a line with slope 1/2 is shown as fully describing all these data, in agreement with the theory of Lake and Thomas. One important feature of the G'' and τ correlation must be noted. This is the unusual ordering of loss modulus with respect to cross-link density. Of the various viscoelastic functions previously presented, only G'' fails to show inverse proportionality with cross-link density in the terminal region. It should also be noted that the tear energy master curves behave as G'' when the corresponding states reference temperatures are used (figure not given in paper). An alternate correlation of the

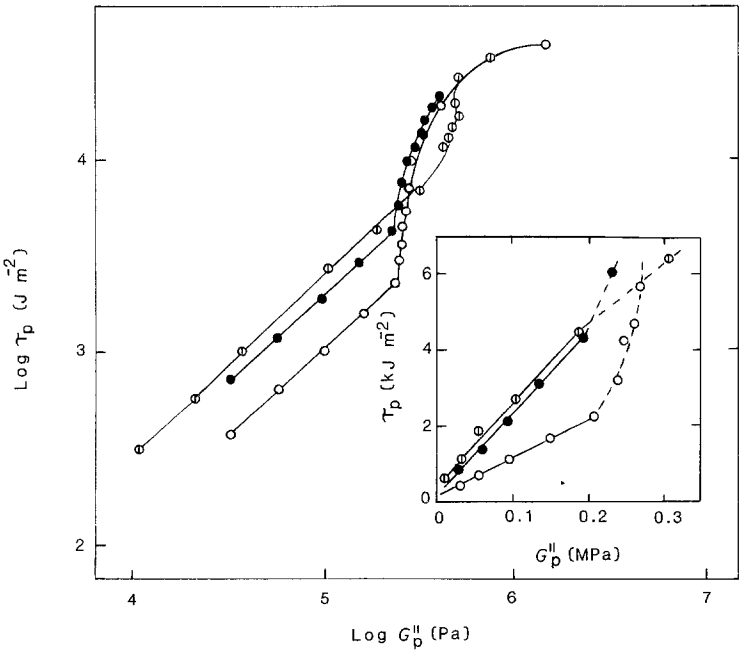

Figure 12 Reduced tear energy τ_p, as a logarithmic function of logarithmic reduced shear loss moduli, G''_p, at corresponding times for (○) HTPB-1, (●) HTPB-2, (⊖) HTPB-3. Inset: data in correlated region replotted linearly.

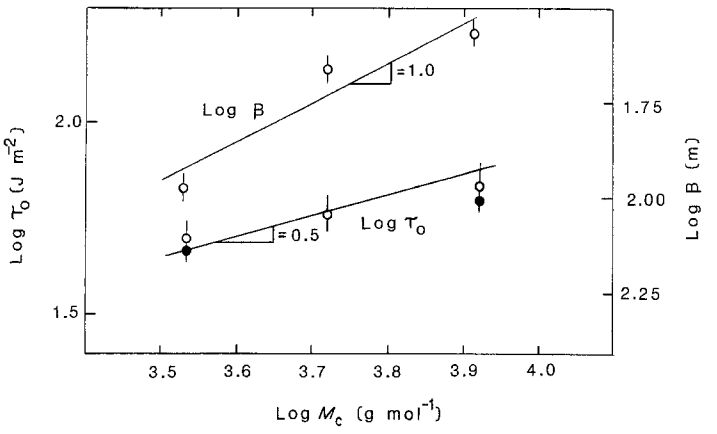

Figure 13 Logarithmic plots of the threshold tear energy τ_0, from extrapolation and measurement, and the slope, β, of tear energy plotted against loss moduli correlation as functions of average molecular weight between effective cross-link sites, $M_c^{\frac{1}{2}}$. (○) From G_p'' correlation, (●) threshold tear.

tear data with the retardation function L is under development.

As was previously mentioned, unstable tearing was observed for these elastomers in the vicinity of the intermediate tear energy plateau. Unstable tearing is a complex phenomenon displayed by many elastomers. During unstable tearing, the tear does not propagate at a steady rate, but, rather initiates and arrests at fairly regular intervals. Correspondingly, the observed force necessary to propagate the tear varies widely from a minimum at tear arrest to a maximum at tear initiation. Previous work [19, 33] indicates that this behaviour can lead to misleading measurements of tear energy. In order to determine whether the plateau was an inherent property of the polymer network or an anomalous test result, additional tests were performed on the tightest network. Because different lots of raw ingredients were used, and a double-notched specimen was employed in an attempt to minimize unstable tearing, this network was designated HTPB-1*. Fig. 14 shows the tear energy master curve for HTPB-1* with the samples experiencing unstable tearing highlighted as solid symbols. As can be seen, the region of unstable tearing is contained within the intermediate plateau, and begins at the point where the correlation between G_p'' and τ_p ends.

Fig. 15 presents the region of unstable tearing for this elastomer in terms of strain rate plotted against inverse absolute temperature. At the highest strain rate this region was bounded by 20 and $-40°$ C. The time-dependent nature of this tearing phenomenon is illustrated by the shift of this region to lower temperatures at lower rates. The slopes of the boundary lines were drawn to agree with the shift factors in Fig. 5. It can be seen from this presentation that the same Arrhenius shift factors that describe the viscoelastic response of this polymer network also describe the time-dependent nature of unstable tearing. Similar treatment of the time-dependent nature of unstable tearing has recently been discussed for a series of elastomers [34]. Finally, the unstable tearing data in Fig. 14 was reduced using the tear arrest force. Use of the force minimum was shown previously to be an unbiased estimator of tear energy in the absence of unstable tearing [33]. Because the region of unstable tearing corresponds to the same underlying viscoelastic time scale as the creep data, and the tear energy utilized in this region provides a good estimate of

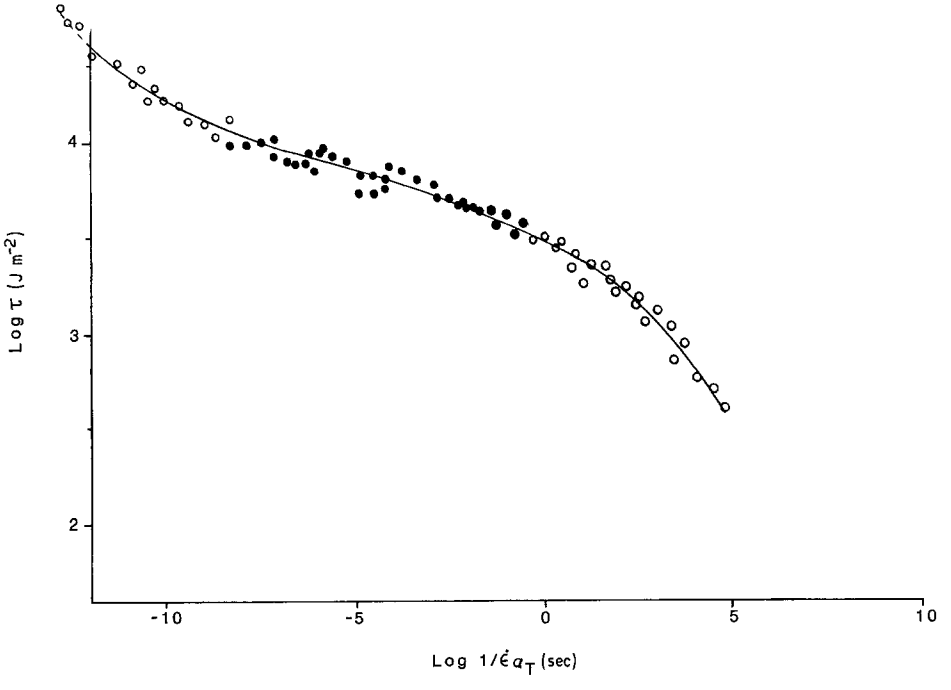

Figure 14 Log tear energy, τ, plotted against log reduced inverse strain rate, $1/\dot{\epsilon}a_T$, for HTPB-1. (○) Stable, (●) unstable.

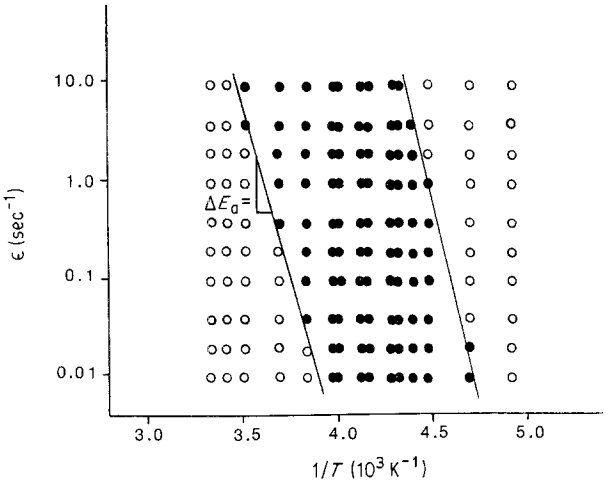

Figure 15 Region of unstable tearing for HTPB-1 in terms of strain rates, $\dot{\varepsilon}$, and inverse absolute temperature. (○) Stable, (●) unstable.

stable tearing, it is concluded that the intermediate tear energy plateau is an inherent feature of the network polymer.

3.3. Comparisons between different elastomers

The logarithm of the reduced shear creep compliance of several elastomers are compared at 0° C in Fig. 16 as a function of the logarithmic reduced time scale log t/a_T. HTPB-2 represents the urethane–cross-linked polybutadiene elastomers. A randomly cross-linked fluorinated hydrocarbon elastomer VITON represents a well-behaved series of elastomers which have already been described as part of this study [10]. The creep response of two polybutadiene elastomers cross-linked with different concentrations of dicumyl peroxide PB-1 and PB-2 are also shown, as well as that of sample HTSBR, a styrene–butadiene copolymer similar to the HTPB series of elastomers.

The equilibrium shear compliances J_e indicated at long times are all about 1.0×10^{-6} Pa^1 except for that of the PB-1 sample which is unexpectedly somewhat higher. The fact that the PB-1 softening dispersion is found at shorter times than that of the PB-2 elastomer has to be attributed to its higher *cis* to *trans* ratio of placements, 0.80 as opposed to 0.67, which reflects a lower T_g. The fact that the rate of creep of the VITON elastomer is approximately five orders of magnitude slower in the softening dispersion than that of the PB-2 we believe is a reasonable reflection of a T_g which is 70° C higher (see Table I).

What is most unexpected is that the softening dispersion of the urethane cross-linked elastomers are found at surprisingly short times; e.g. the intermediate plateau of HTPB-2 is reached near log $t/a_T = -12$ in spite of the fact that its T_g is some 13° C higher than that of the PB-2 material. Yet the latter's intermediate plateau is approached at about log $t/a_T = -6$; some seven orders of magnitude later. Hence the material which is further above its T_g creeps slower in the softening zone.

However, if the creep compliance curves are compared at their respective T_gs, we see in Fig. 17 that the softening dispersions are, within experimental uncertainty, at the same place in the time scale of response. Specifically the positions of the four $J_p(t)$ curves at a compliance level of 1.0×10^{-8} Pa^{-1} appear to be spread on the time scale by not much more than one decade of time. Relative uncertainties of T_g values of ± 1.5° C can account for this spread in positions. Until more precise relative T_gs can be measured we can tentatively surmise that all polymers creep at the same rate at T_g deep in the softening zone. This conclusion appears reasonable when one considers that short-range chain dynamics should determine both creep rates just above the glassy level as well as changes in local liquid structure, the kinetics of which determine T_g. It is well established that normally in the temperature range from T_g to $T_g + 100$° C the relative degree of crowding and the random fluctuations of the local density on the molecular level are the principal determiners of rate processes in polymers. The usual thermal kinetic energy is available over the entire temperature range for molecular level jumps at the moment and position of a density rarefaction. The *intrinsic* dependence of rate processes in polymers on temperature has yet to be isolated, but is presumed not to be a dominating influence at temperatures no more than 150° C above T_g. The relation between the creep rate and T_g will be critically tested in the future.

Returning to the tear data, Fig. 18 presents the tear master curves for the four elastomers in Fig. 17. All four elastomers have approximately the same apparent cross-link density and are shown reduced to

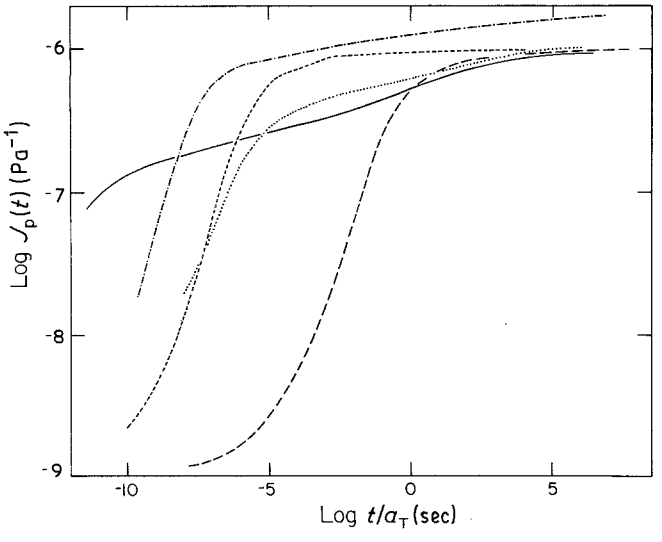

Figure 16 Double logarithmic plot of the reduced shear creep compliance, $J_p(t)$, as a function of reduced time, t/a_T, for five elastomers at $T_0 = 0$° C. (——) HTPB-2, (– – –) VITON, (– – –) PB-2, (– – –) PB-1, (· · ·) HTSBR.

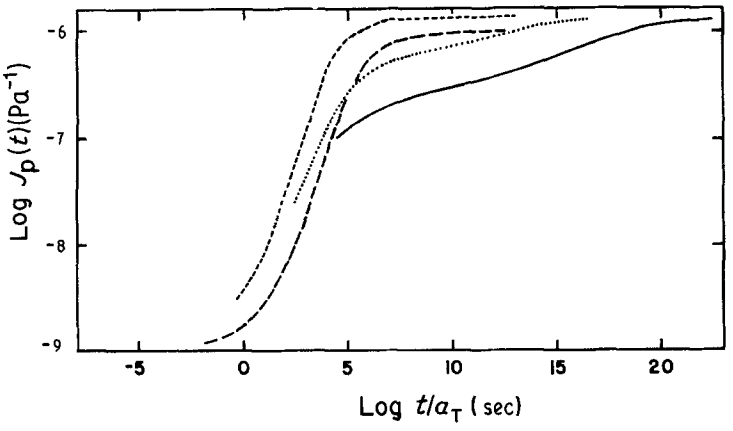

Figure 17 Double logarithmic plot of the reduced shear creep compliance, $J_p(t)$, as a function of reduced time, t/a_T, for four elastomers at T_0 = 0° C. (——) HTPB-2, (— — —) VITON, (– – –) PB-2, (· · · ·) HTSBR. $T_0 = T_g$.

their network T_gs. Because the variables of cross-link density and T_g have been removed, the remaining differences should reflect the influence of other variations in molecular structure, particularly those which lead to dissipative mechanisms. Both of the urethane–cross-linked networks, HTPB-1 and HTSBR, show evidence of an intermediate plateau with greatly enhanced tear resistance. This plateau does not occur in either the randomly cross-linked polybutadiene of similar microstructure PB-2, or in the VITON elastomer. Clearly, the presence of the urethane linkage plays an important role in the resistance to tear for these networks.

Fig. 19 presents the logarithmic time-scale shift factor for the various elastomers. The a_Ts for the peroxide–cross-linked polybutadiene PB-2 and all of the fluorinated hydrocarbon elastomers, the VITONS, show the usual kind of temperature dependence which is describable with the WLF equation. The great sensitivity to volume changes near T_g diminishes considerably with increasing temperature and hence increasing specific volume. However, a strong dependence on temperature is maintained even above T_g + 100° C by the HTPB elastomers. This explains the position inversion along the time scale observed in Fig. 16 where T_0 = 0° C. The apparent activation energies for the HTPB series are, in ascending order, 42 kcal gmol^{-1} (0.176 MJ gmol^{-1}) for HTPB-3, 46 kcal gmol^{-1} (0.193 MJ gmol^{-1}) for HTPB-1, and 52 kcal gmol^{-1} (0.218 MJ gmol^{-1}) for HTPB-2. As can be seen, the values are out of order relative to the cross-linking level. The same kind of Arrhenius temperature dependence was observed for the urethane end-linked SBR elastomer with an apparent activation energy at 43 kcal gmol^{-1} (0.180 MJ gmol^{-1}). No significant difference has been found in the T_g of these samples. Therefore, normally no difference in temperature dependence would be expected.

Evidence of hydrogen bonding in these urethane–cross-linked elastomers was obtained from infrared analysis of HTPB-1. By comparing the areas under the peaks and extinction coefficients for the hydrogen bonded N–H group (3310 cm^{-1}) and the free N–H group (3440 cm^{-1}) peaks, it was found that greater than 80% of the N–H groups were hydrogen bonded [35]. The appearance of the intermediate plateau in both the creep compliance and the tear energy master curves, the Arrhenius shifting behaviour, and the enhanced tear resistance are very interesting phenomena that appear to be related to the presence of the hydrogen bonded, highly polar urethane linkages. These phenomena indicate the existence of energy dissipation mechanisms which are not available to elastomeric networks cross-linked by other methods. Using linear viscoelastic stress analysis, Radok and Tai [36] have shown that the inclusion of a second phase domain in an elastomeric material will enhance the ability of the material to dissipate energy, even if the domain is perfectly elastic. It is therefore surmised that a microphase of urethane segments exist in the urethane–cross-linked elastomers used in this study and that these segments are responsible for the

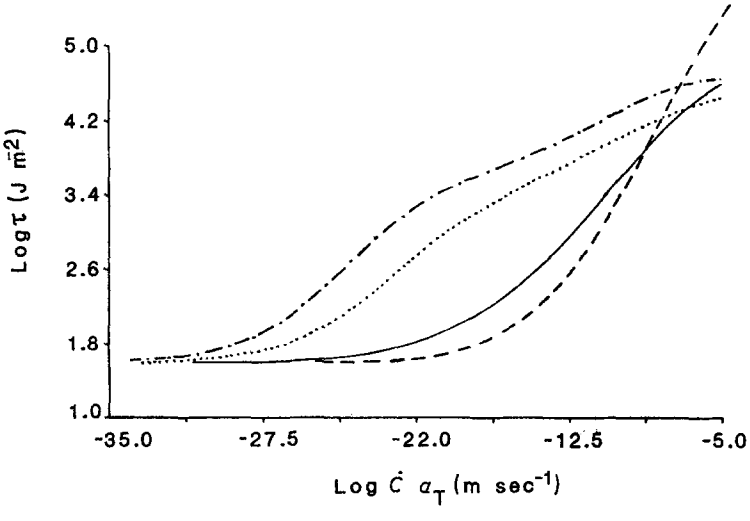

Figure 18 Logarithmic tear energy, τ, as a function of log reduced tear rate, $\dot{C}a_T$, for four elastomers at T_0 = 0° C. (– – –) HTPB-1, (· · · ·) HTSBR, (——) VITON, (– – –) PB-2. $T_0 = T_g$.

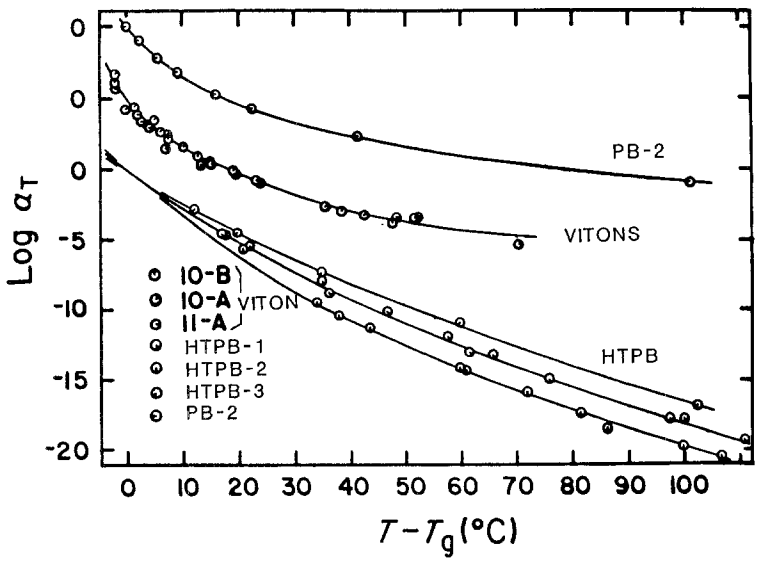

Figure 19 Logarithmic time scale shift factors presented as functions of the temperature difference $T-T_g$ for seven elastomers.

distinctive time-dependent viscoelastic and tearing behaviour. The existence of this second phase does not appear to have affected the thermorheologically simple nature of these elastomers.

4. Conclusions

1. Three points of correspondence have been identified between time-dependent viscoelastic functions and tear energy for a series of urethane–cross-linked elastomers. The first is an inverse proportionality in the terminal region between cross-linked density and both torsional creep and tear energy data, with the looser network being more dissipative and displaying the greatest resistance to tear. Secondly, master curves of both creep compliance and tear energy exhibited a unique intermediate plateau. This plateau measured approximately 13 decades in time in each case. Finally, in the terminal or long time region, it was found that the dynamic loss modulus G'' could be linearly correlated with the tear energy.

2. The inverse proportionality in the terminal region between cross-link density and the various viscoelastic functions studied was not observed for G''. This viscoelastic loss function did not display a distinct ordering with respect to cross-link density.

3. The origin of the intermediate plateau in both creep compliance and tear energy master curves is believed to be related to the nature of the cross-linking system. A polybutadiene elastomer of identical microstructure, randomly cross-linked to the same apparent level with dicumyl peroxide, showed no evidence of a plateau. Additionally, the urethane cross-links are believed to be responsible for the unusual Arrhenius-type time-temperature shifting behaviour observed. It is surmised that hydrogen-bonded domains of urethane segments are responsible for this distinctive behaviour.

4. Unstable tearing of the elastomers was observed only in the region of this intermediate plateau. It has been shown that the region of unstable tearing is itself a time-dependent phenomenon which is described by the same time–temperature shift coefficients as the small deformation response data. It has also been shown that the tear energy plateau is related to structural features within the network, and does not depend upon stable tearing.

5. The slope of the G'' against τ linear relationship was found to be dependent on cross-link density with the looser networks having higher slopes. It has been suggested that this slope variation is associated with changes in tear tip diameter at the different cross-linking levels. Extrapolation of the G'' against τ relationship to $G'' = 0$ provided an estimate of tear resistance in the absence of viscoelastic dissipation. These extrapolated tear energies τ_0 were found to agree well with tear energies measured under threshold conditions. The dependency of these τ_0 values on the average molecular weight between cross-link junctions M_c was found to be adequately described by a 1/2 power, in agreement with the Lake and Thomas theory. At short times, G'' was found to be uncorrelated with τ. In this region, tear energy increased more rapidly than would be expected from the loss modulus data. The transition between correlated and uncorrelated regions was related to the intermediate plateau observed.

Acknowledgements

This work was supported by a grant from the Air Force Office of Scientific Research. The assistance of R. H. Seiple in the performance of some of the tear tests is greatly appreciated.

References

1. H. W. GREENSMITH and A. G. THOMAS, *J. Polym. Sci.* **18** (1955) 189.
2. L. MULLINS, *Trans. Inst. Rubber Ind.* **35** (1959) 213.
3. K. A. GROSCH, J. A. C. HARWOOD and A. R. PAYNE, *Nature* **212** (1966) 497.
4. R. F. LANDEL and R. F. FEDORS, "Fracture Processes in Polymeric Solids" (Interscience-Wiley, New York, 1965).
5. E. H. ANDREWS, *J. Mater. Sci.* **9** (1974) 887.
6. A. N. GENT, "Science and Technology of Rubber" (Academic, New York, 1978).
7. A. KADIR and A. G. THOMAS, *Rubber Chem. Technol.* **54** (1981) 15.
8. A. AHAGON and A. N. GENT, *J. Polym. Sci. Polym. Phys. Edn* **13** (1975) 1903.
9. H. K. MUELLER and W. G. KNAUSS, *Trans. Soc. Rheol.* **15** (1971) 217.
10. D. J. PLAZEK, I.-C. CHOY, F. N. KELLEY, E. VON MEERWALL and L.-J. SU, *Rubber Chem. Technol.* **56** (1983) 866.

11. D. J. PLAZEK, *J. Polym. Sci. A-2* **6** (1968) 621.
12. E. F. CLUFF, E. K. GLADDING and R. PARISER, *J. Polym. Sci.* **45** (1960) 341.
13. E. RIANDE, H. MARKOVITZ, D. J. PLAZEK and H. RAGHUPATHI, *J. Polym. Sci. C* **50** (1975) 405.
14. S. J. ORBON, PhD thesis, University of Pittsburgh (1978).
15. J. D. FERRY, "Viscoelastic Properties of Polymers", 3rd Edn (Wiley, New York, 1980).
16. D. J. PLAZEK, *J. Polym. Sci. A-2* **4** (1966) 745.
17. P. THIRION and R. CHASSET, "Proceedings of the Conference on Physics of Non-Crystalline Solids" (North-Holland, Amsterdam, 1965).
18. E. PASSAGLIA and G. M. MARTIN, *J. Res. N.B.S. Phys. Chem.* **68A** (1964) 519.
19. A. N. GENT and A. W. HENRY, *Proc. Inst. Rubber Ind.* **193** (1967).
20. J. GLUICKLICH and R. F. LANDEL, *J. Appl. Polym. Sci.* **20** (1976) 212.
21. S. J. BENNETT, G. P. ANDERSON and M. L. WILLIAMS, *ibid.* **14** (1970) 735.
22. N. E. KING and E. H. ANDREWS *J. Mater. Sci.* **13** (1978) 1291.
23. H. W. GREENSMITH, L. MULLINS and A. G. THOMAS, *Trans. Soc. Rheol.* **4** (1960) 179.
24. G. J. LAKE and A. G. THOMAS, *Proc. R. Soc. London Ser. A* **300** (1967) 1460.
25. F. BUECHE, "Physical Properties of Polymers" (Wiley, New York, 1962).
26. L. MULLINS, (ed.) "Proceedings of Natural Rubber Products Research Association," Jubilee Conference, Cambridge, 1964, (McLaren, London, 1965).
27. T. L. SMITH and W. H. CHU, *J. Polym. Sci. A-2* **10** (1972) 133.
28. A. N. GENT and R. H. TOBIAS, *ibid.* **20** (1982) 2051.
29. R. H. TOBIAS, PhD dissertation, University of Akron (1982).
30. H. W. GREENSMITH, *J. Appl. Polym. Sci.* **3** (1960) 183.
31. A. G. THOMAS, *J. Polym. Sci.* **18** (1955) 177.
32. A. L. KINLOCH and R. J. YOUNG, "Fracture Behavior of Polymers" (London, 1983).
33. R. G. STACER, L. C. YANYO and F. N. KELLEY, *Rubber Chem. Technol.* **58** (1985) 421.
34. R. G. STACER and F. N. KELLEY *Rubber Chem. Technol.*, in press.
35. L.-J. SU, PhD dissertation, University of Akron (1984).
36. J. R. M. RADOK and C. L. TAI, *J. Appl. Polym. Sci.* **6** (1962) 518.

Received 8 April
and accepted 29 June 1987